Bulletin of Electrical Engineering and Informatics
Vol. 12, No. 4, August 2023, pp. 2041~2048
ISSN: 2302-9285, DOI: 10.11591/eei.v12i4.4722

The one-phase $SrMg_2La_2W_2O_{12}:Tb^{3+}$, Sm^{3+}, Tm^{3+} phosphor and its optical features in multicolor and white-illumination LEDs

Ha Thanh Tung[1], Huu Phuc Dang[2], Phung Ton That[3]
[1]Faculty of Basic Sciences, Vinh Long University of Technology Education, Vinh Long Province, Vietnam
[2]Faculty of Fundamental Science, Industrial University of Ho Chi Minh City, Ho Chi Minh City, Vietnam
[3]Faculty of Electronics Technology, Industrial University of Ho Chi Minh City, Ho Chi Minh City, Vietnam

Article Info

Article history:

Received Sep 7, 2022
Revised Dec 16, 2022
Accepted Jan 11, 2023

Keywords:

Color homogeneity
Luminous flux
Monte Carlo theory
$SrMg_2La_2W_2O_{12}$
White light-emitting diode

ABSTRACT

Researchers propose the phosphors emit many colors $SrMg_2La_2W_2O_{12}:Tb^{3+}$, Sm^{3+}, Tm^{3+} (SMLLW:RE^{3+}) (RE^{3+}=Tb^{3+}, Sm^{3+}, Tm^{3+}) synthesized using the solid-status reacting technique as promising downward-transformation luminous substances for diodes emit white illumination and screens in the current study. The structural and binding data given by X-ray diffraction (XRD) data and fourier transform infrared (FTIR) spectroscopy suggest the corresponding orthorhombic configuration and vibrational powers, respectively. The stimulation and radiation bands of color of SMLLW:RE^{3+} phosphor show that such phosphors may be successfully stimulated via ultraviolet (UV) illumination and generate green, orange-red, and blue (stands for G, O-R, B) illumination, in turn. For different doses of the triggers Tb^{3+}, Sm^{3+}, and Tm^{3+} within the SMLW phosphor base, luminescence, decomposition periods, Commission Internationale De L'eclairage (CIE) color coordination, along with correlated hue heats (T_{cct}) are specified. When a triple-doped SMLW phosphor is activated using a ligand-to-metal charge transition (LMCT), it produces G, O-R, B hues at the same time and can be adjustable to white light, according to the results. An effective power transfer among rare-earth ions was found and investigated using decay curve analysis. According to the findings, SMLW:RE^{3+} (RE=Tb, Sm, Tm) are suitable options to use for light-emitting diodes (LEDs) and screens creation.

Corresponding Author:

Huu Phuc Dang
Faculty of Fundamental Science, Industrial University of Ho Chi Minh City
No. 12 Nguyen Van Bao Street, Ho Chi Minh City, Vietnam
Email: danghuuphuc@iuh.edu.vn

1. INTRODUCTION

Systems and displays for white illumination, which have been a part of everyday life, have received a great deal of attention recently [1]. They are regarded as crucial components of the human/electronic interface. To achieve white illumination radiation in light-emitting diodes (LEDs) and screens, simultaneous radiation of red-green-blue (RGB) hues is required. The usage of white light-emitting luminous substances in radar or plasma displays, sensors, and white LED (WLED) lamps has increased their significance [2]. The phosphors used for screens need to meet the criteria such as: i) significant efficacy of quantum; ii) significant color rendering index (CRI); iii) long lifespan; iv) adequate afterglow (pertinacity); and v) a wider chromatic range. The chromatic scale reflects the whole chromatic assortment formed by several main sources for the purpose of displaying beautifully saturated chromas [3]. Owing to their *f—f* or *d—f* transformations, luminous substances containing trivalent rare-earth (RE^{3+}) ions are widely known to be a significant part of the

displays and signage fields [4], [5]. Lanthanides, on the other hand, have low fluorescence quantum yields caused by narrow stimulation apexes as well as limited absorption.

It is possible to solve the foregoing issue through using ligand sensitization alongside lanthanide ions. The ligand (a particle that binds the center metal atom) takes in the incident light, then passes excitation power towards the lanthanide ion so that it can undergo fluorescence. Solely in the case of the ligand having a wide absorptivity cross-section, the brightness for the lanthanide ion under said stimulation becomes superior to the brightness of the lanthanide ion with direct stimulation, a wider stimulation range, and a beneficial power transmission speed to the lanthanide ion. Furthermore, the insertion of various non-fluorescent compounds (such as Y^{3+}, Gd^{3+}, or La^{3+}) in the non-organic host through intramolecular power shift [6] can boost strength even further. The host materials used in screens must meet certain criteria, including: i) elevated dopant dissolution; ii) the presence of a stimulation range in the ultraviolet (UV) area; iii) the ability to excite various active ions under the identical stimulation wavelength; iv) effective non-radiative energy shift towards the said ions; and v) superior reliability of chemical. Inorganic phosphor substances composed of ions with a valence of three (RE^{3+}) typically have highly strong UV absorbing ranges since to allowed intra-configurational $4f^{n} \rightarrow 4f^{n-1}\ 5d$ shifts as well as the charge transfer ligand-to-metal charge transition (LMCT) shift between ligand and metal responsible for hiding the forbidden thin intra-configurational $4f^{n} \rightarrow 4f^{n}$ shifts [7]. The UV absorbing ranges of LMCT are capable of absorbing photons over a broad wavelength range. As a result, the LMCT state is critical for the wavelength sensitivity of whole RE^{3+} ions [8]. The writers evaluated the stated outcomes according to tungstate families and discovered just some illumination investigations including these substances [9]. Lanthanum-based tungstate phosphors are simple to make, they also have a wide range of uses, including phosphors, optic fibers, scintillators, and laser host substances. As a result, the writers selected a lanthanum-based tungstate combination like a host substance. Based on their photoluminescence (PL), a variety of RE substances with elevated quantum effectiveness and diverse spectral ranges are commonly utilized for cathodoluminescence, display phosphor screens, lasers, and lamps [10]. Since the concurrent radiation of main colors is required for white light creation, many RE^{3+} ions are required for combined white lighting radiation [11]–[13]. Tb^{3+}, Sm^{3+}, and Tm^{3+} ions are among the RE^{3+} ions that may be co-doped in phosphor host substance to provide effective white illumination radiation. Tb^{3+} is a key activator ion found within phosphors to be utilized in displays with even surface, three-chroma fluorescent lights, yellow-green tubes as well as displays based on amplifying x-ray [14]. Its radiation is mostly between $^5D_4$ and $^5D_3$ states and a ^7F_J (J=6, 5, 4, 3) multiplet inside the $4f^8$ structure, with Tb^{3+} radiation strengths varying with dopant concentration. When examining the fluorescence from its producing $^4G_{5/2}$ level, the Sm^{3+} ($4f^5$) ion would be among the most fascinating RE^{3+} ions as well, exhibiting relatively high quantum effectiveness and establishing a feasible viewpoint for illumination and screens [15]. Tm^{3+} ($4f^{12}$) ions, while not as effective in terms of radiation quantum efficiencies, do contribute significantly to the radiation of one of the main hues, blue, which is highly valuable in the strong white illumination creation. As a result, the RE^{3+} ions (Tb^{3+}, Sm^{3+}, and Tm^{3+}) exhibit line-like and strong stimulation ranges in the close UV area, as well as intriguing radiation tendency within the green, red-orange as well as blue areas; such ions were implemented in the hosts of $SrMg_2La_2W_2O_{12}$ (SMLW) after crystallization for the purpose of determining how the rare earth concentration influence the white illumination creation. To identify the impact of co-doped ions, a SMLW host was lately utilized to co-dope Tb^{3+}/Eu^{3+} or Dy^{3+}/Tm^{3+} [16], [17].

In light of the foregoing, the current study was intended for the investigation concerning the illumination mechanic of co-doped RE^{3+} ions (RE^{3+}=Tb^{3+}, Sm^{3+}, and Tm^{3+}) in SMLW host (complicated perovskite formation). The distinctive green radiation for Tb^{3+}, the bright orange-red radiation of Sm^{3+}, along with the blue-color radiation for Tm^{3+} generated through SMLW sample all contain the unusual property in producing multiple color mixtures when exposed to UV light. Transfer of power in LMCT state to the active ions, as well as radiative and non-radiative transitions concerning the functioning ions, are used for the task of clarifying brightness improvements and extinguish processes in phosphors using various quantities of active ions. This makes a contribution for the radiation of different hues across a broad hue gamut. We determined the luminous feature in the produced phosphors utilizing a commission internationale de l'eclairage (CIE) chroma diagram under varied stimulation wavelengths as well as distinct mixtures containing the active ions via collecting the PL bands of color. Luminosity's color tuning was also studied using optimal mixtures of Tb^{3+}, Sm^{3+}, and Tm^{3+} ions.

2. METHOD

We created and treated the SMLW phosphors with Tb^{3+}, Sm^{3+}, and Tm^{3+} (SMLW:TbSmTm) using a solid status technique under great temperature accompanied by various mixtures as well as dopants' concentrations. Greatly clear $SrCO_3$, La_2O_3, WO_3, $MgCO_3$, Tb_4O_7, Tm_2O_3, and Sm_2O_3 were employed as

initial ingredients. The raw components were combined in stoichiometric amounts corresponding to expression (1) [18], [19].

$$SrCO_3 + 2MgCO_3 = \left(1-(x+y+z)\right)La_2O_3 + 2WO_3 + \frac{x}{2Tb_4O_7} + ySm_2O_3 + zTm_2O_3 \rightarrow SrMg_2La_{2(1-(x+y+z))}W_2O_{12}:Tb_{2x},Sm_{2y},Tm_{2z} \rightarrow 3CO_2 \uparrow \quad (1)$$

The necessary quantities of beginning ingredients, around 7 g, were put inside one agate mortar and pulverized with acetone. The pulverized outcome was placed in one silica crucible for 6-hour sintering at 1,200 °C. The thermal-treated specimens were pulverized one more time for further characterization. A powder x-ray diffractometer fitted with a curving location-sensitive detector was used to study the crystal layout of the phosphors, and information was gathered utilizing Co-Kα radioactivity for wavelength 1.788 97. Perkin elmer spectrum 1 fourier transform infrared (FTIR) spectrometer was used to perform fourier transform spectroscopic investigation of pressed KBr disks in the 500–4,000 cm^{-1} range. At room temperature, we evaluated the PL as well as photoluminescence stimulation (PLE) using one spectrofluorometer containing 450 W xenon light for stimulation. We securely squeezed the undoped and doped powders in the spectrofluorometer's solid sample container to be irradiated at an angle of 15° angle. We captured the PL in the form of a reflection. We obtained the luminescence decay curves via stimulating the powder specimens using one 35 W xenon flashlight.

3. RESULTS AND DISCUSSION

When there is a 3,000-K correlated color temperature (CCT), choosing a red-illuminating supply within 605-615 nm and a green illumination supply between 530 and 545 nm gives a fairly limited band that exhibits a color quality scale (CQS) value of 70 (an undesirable result when it comes to typical illuminating implementations). A line edge roughness (LER) value of 400 lm=W may be achieved inside the stated range, roughly the maximum result attained in a white illumination. Under the 4,500-K CCT value, the outcomes appear to be similar, accompanied by the same CQS as well as a minimally inferior LER, caused by the significantly stronger influence from the blue radiation band. Our eyes are less receptive to this band. Because it appears that adequate chroma generation is unobtainable using one insignificant proportion for narrow radiation apexes, the employment of *4f–4f* band dischargers is not effective to create significant chroma generation illuminating implementations. On the other hand, it is possible to achieve significant results of LER, making them an excellent option to be utilized in displays like LCDs, in which it is possible for LEDs to be utilized as backlights. The main chromas' saturation is the sole concern in this situation [20]–[22].

This limits the kind of dopants that can act as good materials for WLEDs. Rare-earth line emitters, like Eu^{3+}, Sm^{3+}, or Tb^{3+} exhibit only thin *4f–4f* stimulation bands within the region between close-UV and blue in the bands of color. Charge transition states (CTS) along with the 5d states would be typically seen under greater power, such as those found in fluorescent lights, just like previously indicated. As an example, Eu^{3+} possesses stimulation lines between 394 and 465 nm, they appear to be relevant for pumping. Nevertheless, the lines' breadth in the stimulation bands of color is frequently significantly narrower compared to the width of the lines in the pumping LED, decreasing overall converting effectiveness. This is particularly difficult in the close-UV pumping LEDs situation; it must convert the whole output photons. Moreover, small heat or current-dependent changes in the LED's emitting bands of color might result in variations in the phosphor's illumination output because of the changes in the intersection of the spectrum. The shifts of the excitation spectrum in the phosphor may also alter the intersection with the LED's output. For example, if pumped under 405 nm (on the rim of the charge transition stimulation range as well as not harmonizing in inner *4f–4f* shifts in Eu^{3+}), $La_2O_2S:Eu^{3+}$ has a 60% more elevated illumination productivity at 120 ºC compared to normal heat. Thermal expansion of this range enhances the overlap with the excitation source, resulting in a rise in illumination production, which counteracts the 'usual' thermal quenching behavior. When used for LEDs, every phosphor has elevated exterior quantum effectiveness permits for the employment of a little phosphor substance quantity above the LED chip. It reduces the absorbing losses caused by the downward-transformed illumination. As a result, dopant ions possessing significant absorption cross-sections, which include Eu^{2+} as well as Ce^{3+}, are preferable to band-discharging rare-earth ions, with poor absorbing intensities in the *4f–4f* shifts. By lowering the stimulation density, distinct packaging with a distant phosphor film may avoid these consequences. Because the decay times of the wideband emission ions Eu^{2+} and Ce^{3+} are in the hundreds and tens of nanoseconds ranges, no saturation is expected. Because the decay duration of numerous *4f–4f* line emitters, such as Eu^{3+} or Tb^{3+}, is only a few milliseconds, saturation impacts are feasible in this situation as well [23]–[25].

Because of the cleavage in the 5d stimulated level by the crystal structure, along with the multiplet cleavage in the $4f^6$ configurations, the stimulation bands of color for Eu^{2+} doped materials are wide and

generally nothing special. The second one appears to be analogous to the basic status cleavage of the ^7F_J states in Eu^{3+}, occasionally resulting in a fine structure with a staircase form for the excitation spectra. A great overlap in close-UV and blue pumping LEDs is available for green to red producing phosphors. Numerous trivalent rare-earth ions (except Ce^{3+}) generate a number of rather narrow radiation lines because of intrinsic *4f-4f* transitions. This type of transition is not affected by the host chemical significantly. Nevertheless, the host picks principles relating to the local symmetries, crystal field splitting, and quantum performance of *4f - 4f* dischargers through the non-radioactive channels in addition to heat absorption to decide the relative strength in the radiation ranges. Among such rare-earth ions, many emit observable light. Specifically, noteworthy rare-earth ions shown to be advantageous in fluorescence illumination phosphors or cathode ray tubes are Tb^{3+} (green radiation, primary apex under 545 nm) as well as Eu^{3+} (orange-red radioactivity, primary apex at around 600 or 620 nm). Since the 5d states and the CTS are frequently found far below 350 nm, the primary challenge in conveying the chemicals to LED implementations would be the inefficient broadband excitation within the spectrum region between n-UV and blue. WLEDs with poor color rendering properties but good illuminating efficiency are possible. Surprisingly, both the necessary red and green elements may be found in the principal Tb^{3+} and Eu^{3+} radiation maxima. Moreover, utilizing red phosphors treated with Eu^{3+} would be favorable since the green phosphor radiation's reabsorption would be prevented. This is an issue with red phosphors made of Eu^{2+}. Rare-earth ions offering observable luminosity, such as Sm^{3+} and Tm^{3+}, have been investigated for LED implementations. Sm^{3+} ($4f^5$) red radiation is distinguished by numerous emitting maximum points at roughly 560, 600, 650, and 700 nm, as well as a *4f–4f* stimulation reaching the highest point at about 405 nm. Tm^{3+} ($4f^{12}$) emits blue light at 450 nm (can be stimulated at 360 nm), but the converting effectiveness is reduced by the competition for infrared emission decomposition routes. The apparent low efficiency of these rare-earth ions, along with the absence of wide range stimulation within the close-UV and blue, leads them to be unsuitable as dopants for LED phosphors.

When green phosphorus SMLW:RE^{3+} is applied in the WLED model, it results in an inverse shift in its concentrations and YAG:Ce^{3+} concentration, depicted by Figure 1 which concerns two different CCT levels: 3,000 K (Figure 1(a)) and 4,000 K (Figure 1(b)). As the phosphor-concentration opposite appears in the WLED structure, the average CCT values are retainable, and the scattering, reflecting, and absorbing characteristics of internally generated light are influenced to create the differences in white-light quality output. In other words, the SMLW:RE^{3+} concentration can change the color quality of WLEDs, meaning that regulating SMLW:RE^{3+} concentration can help modify the chromatic output of WLED equipment. When the SMLW:RE^{3+} presence rose (2-20%) by weight, the YAG:Ce^{3+} presence fell in order to maintain the average CCT states. Said mechanism applies to WLEDs having color temperatures ranging 5,600-8,500 K.

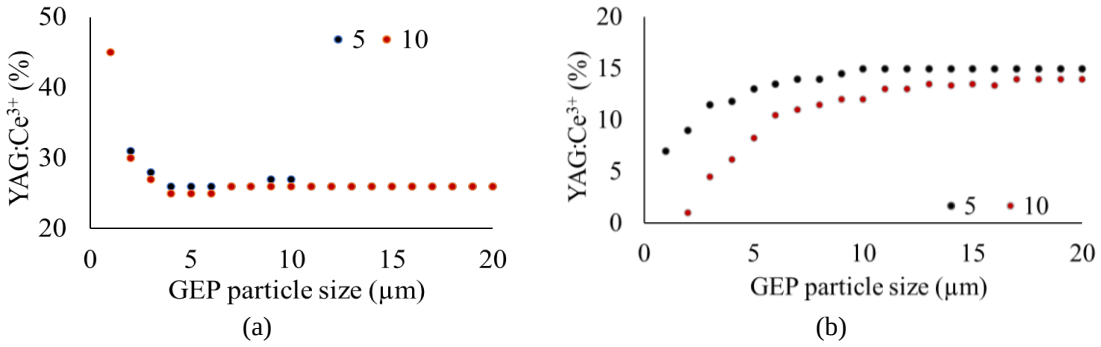

Figure 1. Adjusting phosphor presence to keep median CCT (a) 3,000 K and (b) 4,000 K

The used amount of SMLW:RE^{3+} could be decided with consideration of the application fields. If it requires high and intense luminescence for backlighting, for example, the color rendering feature could be lower. The effect of SMLW:RE^{3+} on the intensity of WLED emission bands was demonstrated in Figure 2, in which white illumination is observed to be comprised of the synthesis of several spectral areas. The depiction was shown regarding CCT of 3,000 K (Figure 2(a)) and 4,000 K (Figure 2(b)). The strength of 420-480 nm as well as 500-640 nm spectra is proportional to the SMLW:RE^{3+} content. As these emitting bands become stronger, the luminance appears to be more intense. Furthermore, there is a surge of blue-illumination dispersion in WLED, indicating the surge of diffusion inside the film of phosphor and the WLED product, favoring chromatic homogeneity. Such an outcome is essential if we utilize SMLW:RE^{3+}. Changing the hue

uniformity in the distant phosphor layout with a good heat can be problematic. Our investigation confirmed that SMLW:RE^{3+}, at poor and elevated hue heats (5,600 K as well as 8,500 K), may augment the WLEDs hue outcome. Thus, the article illustrated the effectiveness for the released illumination of the dual-film remote phosphor layer.

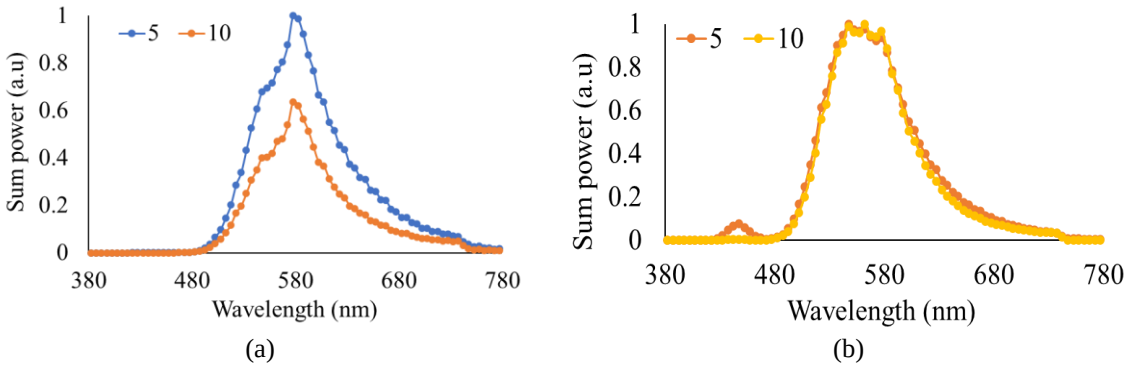

Figure 2. The discharging hue bands in WLED apparatus correlating with SMLW:RE^{3+} presence (a) 3,000 K and (b) 4,000 K

Figure 3 outcomes show that the generated lumen grows dramatically when the concentration of SMLW:RE^{3+} at 2% wt. reaches 20% wt, again under CCTs of 3,000 and 4,000 K in Figures 3(a) and (b). The chromatic divergence was substantially reduced as the said concentration goes down, under every CCT value, as shown by the results from Figure 4, presenting CCT levels of 3,000 and 4,000 K in Figures 4(a) and (b). The outcome may result from the green phosphor layer's absorptivity based on mie-scattering. According to the theory, the blue emission is easily absorbed by the green phosphor particles. The absorbed light is then re-emitted by the phosphors in the emission color of green, owing to the phosphor conversion process. The green particles can absorb the yellow light (emitted by YAG:Ce^{3+}) but because of the longer wavelength of yellow light, the absorption tends to be much weaker, resulting in less yellow light to be converted. So, if the dispersion of blue light is enhanced, it is likely to result in greater absorbed blue light by the green phosphor and consequently greater converted green light amount. The boost of the green light in WLED structures augments the chromatic homogeneity index. Chromatic uniformity is a crucial property for attaining desirable color adequacy of WLEDs. As the chromatic uniformity index becomes greater, the WLED's price increases as well. The advantage of employing SMLW:RE^{3+} would be the inexpensive cost. SMLW:RE^{3+} can thus be widely employed.

To access good color properties of WLEDs, only good color uniformity is insufficient because color uniformity is merely one parameter to examine carefully. With a great hue uniformity rating, hue standards cannot be considered to be good. For the purpose of fully evaluating the color quality of white light from WLED, studies provided the indicators of hue rendering and hue ratio. The hue rendering index defines an object's actual hue when illuminated. The color imbalance is generated when green emission is much more intense than the other blue and yellow emissions. WLED hue accuracy is reduced as a result of this having an effect on the hue standard of WLEDs. According to the results in Figure 5 which exhibits CRI under CCT values of 3,000 and 4,000 K in Figures 5(a) and (b), the CRI somewhat decreased when the remote phosphor SMLW:RE^{3+} film was present. Nevertheless, all of those minor downsides are acceptable. CQS proves to be more useful than CRI, though achieving desirable CQS requires greater efforts [26]–[28]. It would be determined through the following standards: CRI, the desire of the beholder, as well as the chromatic coordinate, making it a genuine indicator that is almost perfect for chromatic-quality assessment. Figure 6 illustrates a rise in CQS, in the case with SMLW:RE^{3+} phosphor sheet, under CCT levels of 3,000 and 4,000 K in Figures 6(a) and (b). Furthermore, when we raised the concentration of SMLW:RE^{3+}, CQS is not changed much with SMLW:RE^{3+} concentrations below 10% wt. When the concentration of SMLW:RE^{3+} becomes greater than 10% wt., not only CRI but also CQS appear to decline considerably. This is caused by the severe waste of chroma in the prevalence of the green color. Thus, before utilizing SMLW:RE^{3+}, it is necessary to pick a suitable concentration.

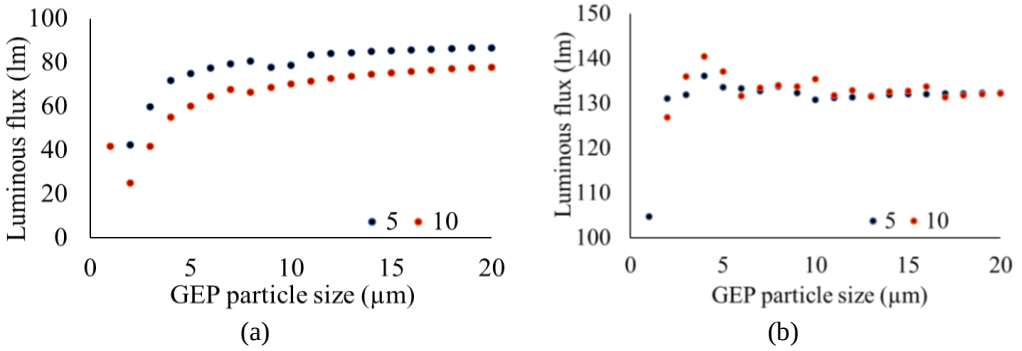

Figure 3. The illuminating beam for WLED apparatus correlating with SMLW:RE^{3+} concentration (a) 3,000 K and (b) 4,000 K

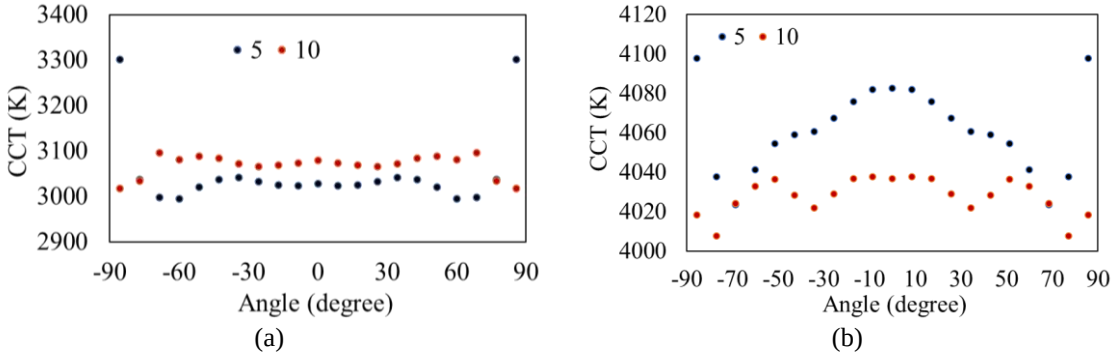

Figure 4. The CCT for WLED apparatus correlating with SMLW:RE^{3+} presence (a) 3,000 K and (b) 4,000 K

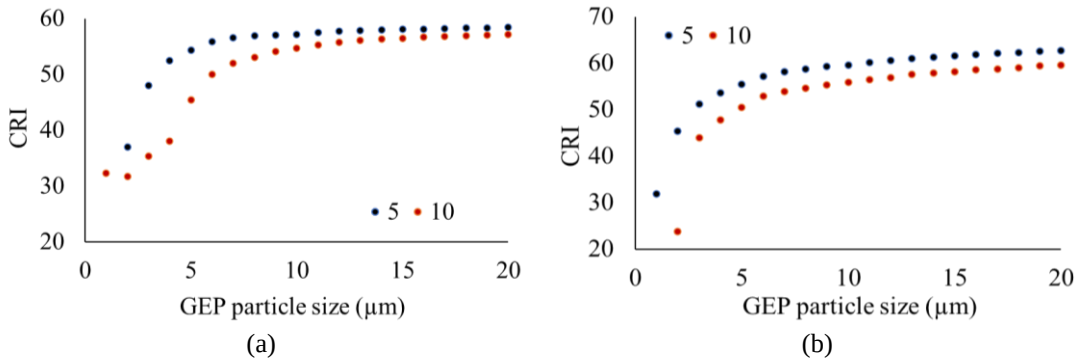

Figure 5. CRI for WLED apparatus correlating with SMLW:RE^{3+} presence (a) 3,000 K and (b) 4,000 K

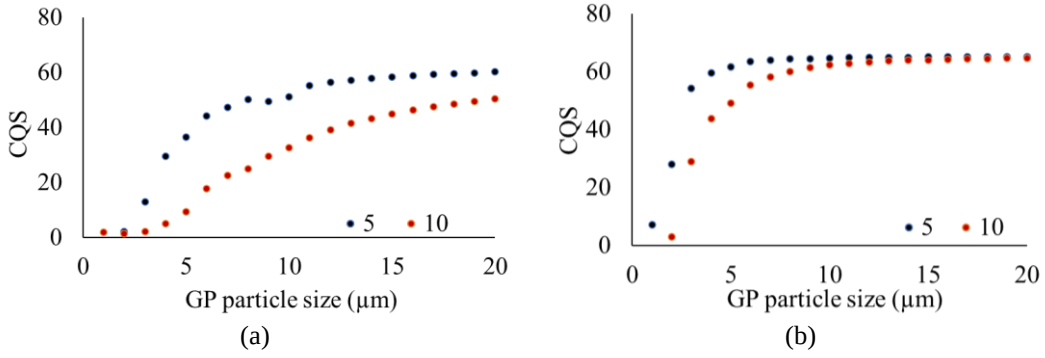

Figure 6. CQS for WLED apparatus correlating with SMLW:RE^{3+} presence (a) 3,000 K and (b) 4,000 K

4. CONCLUSION

The solid-status reaction approach was employed for effectively producing SMLW:Tb^{3+}, Sm^{3+}, and Tm^{3+} phosphors. Phosphors exhibit the typical radiations for Tb^{3+} ($^5D_4 \rightarrow {}^7F_{3-6}$), Sm^{3+} ($^4G_{5/2} \rightarrow {}^6H_{5/2,7/2,9/2}$), as well as Tm^{3+} ($^1D_2 \rightarrow {}^3F_4$, $^1G_4 \rightarrow {}^3H_6$) when exposed to UV illumination and respective *4f-4f* stimulation wavelengths. The fluctuation of radiation strength with rising concentrations was observed in Tb^{3+} and Sm^{3+} co-doped phosphors during the major shifts in Tb^{3+} ($^5D_4 \rightarrow {}^7F_5$) as well as Sm^{3+} ($^4G_{5/2} \rightarrow {}^6H_{7/2}$), accompanied by determining the best proportion of concentration. A shift of power between Tb^{3+} and Sm^{3+} ions, and also between Tb^{3+}, Sm^{3+}, and Tm^{3+} ions, happens via non-radiative mechanisms that can be readily described using a decay curve study. Color chromaticity can be adjusted by changing the dopants, concentration, and stimulation wavelength. When activated by the LMCT band, the integrated illumination of tri-doped SMLW phosphors falls in the "warmer area". In addition to detecting their radiation characteristics, X-ray diffraction (XRD) and FTIR have been used to explore their structural and bonding features. According to the findings of this study, the sample may be recognized as a suitable optic substance when it comes to generating white illumination radiation as well as applying to display implementations.

REFERENCES

[1] T. W. Kang *et al.*, "Enhancement of the optical properties of $CsPbBr_3$ perovskite nanocrystals using three different solvents," *Optics Letters*, vol. 45, no. 18, pp. 4972–4975, Sep. 2020, doi: 10.1364/OL.401058.

[2] G. Prabhakar, P. Gregg, L. Rishoj, P. Kristensen, and S. Ramachandran, "Octave-wide supercontinuum generation of light-carrying orbital angular momentum," *Optics Express*, vol. 27, no. 8, pp. 11547–11556, Apr. 2019, doi: 10.1364/OE.27.011547.

[3] R. Dang, H. Tan, N. Wang, G. Liu, F. Zhang, and X. Song, "Raman spectroscopy-based method for evaluating LED illumination-induced damage to pigments in high-light-sensitivity art," *Applied Optics*, vol. 59, no. 15, pp. 4599–4605, May 2020, doi: 10.1364/AO.379398.

[4] Z. Huang *et al.*, "Towards an optimum colour preference metric for white light sources: a comprehensive investigation based on empirical data," *Optics Express*, vol. 29, no. 5, pp. 6302–6319, Mar. 2021, doi: 10.1364/OE.413389.

[5] S. Ma, P. Hanselaer, K. Teunissen, and K. A. G. Smet, "Effect of adapting field size on chromatic adaptation," *Optics Express*, vol. 28, no. 12, pp. 17266–17285, Jun. 2020, doi: 10.1364/OE.392844.

[6] P. Kaur, Kriti, Rahul, S. Kaur, A. Kandasami, and D. P. Singh, "Synchrotron-based VUV excitation-induced ultrahigh quality cool white light luminescence from Sm-doped ZnO," *Optics Letters*, vol. 45, no. 12, pp. 3349–3352, Jun. 2020, doi: 10.1364/OL.395393.

[7] D. Yan, S. Zhao, H. Wang, and Z. Zang, "Ultrapure and highly efficient green light emitting devices based on ligand-modified CsPbBr 3 quantum dots," *Photonics Research*, vol. 8, no. 7, pp. 1086–1092, Jul. 2020, doi: 10.1364/PRJ.391703.

[8] D. Molter, M. Kolano, and G. von Freymann, "Terahertz cross-correlation spectroscopy driven by incoherent light from a superluminescent diode," *Optics Express*, vol. 27, no. 9, pp. 12659–12665, Apr. 2019, doi: 10.1364/OE.27.012659.

[9] A. Ali *et al.*, "Blue-laser-diode–based high CRI lighting and high-speed visible light communication using narrowband green-/red-emitting composite phosphor film," *Applied Optics*, vol. 59, no. 17, pp. 5197–5204, Jun. 2020, doi: 10.1364/AO.392340.

[10] S. Beldi *et al.*, "High Q-factor near infrared and visible Al_2O_3-based parallel-plate capacitor kinetic inductance detectors," *Optics Express*, vol. 27, no. 9, pp. 13319–13328, Apr. 2019, doi: 10.1364/OE.27.013319.

[11] C.-H. Lin *et al.*, "Hybrid-type white LEDs based on inorganic halide perovskite QDs: candidates for wide color gamut display backlights," *Photonics Research*, vol. 7, no. 5, pp. 579–585, May 2019, doi: 10.1364/PRJ.7.000579.

[12] W.-Y. Chang, Y. Kuo, Y.-W. Kiang, and C. C. Yang, "Simulation study on light color conversion enhancement through surface plasmon coupling," *Optics Express*, vol. 27, no. 12, pp. 629–642, Jun. 2019, doi: 10.1364/OE.27.00A629.

[13] X. Xi *et al.*, "Chip-level Ce:GdYAG ceramic phosphors with excellent chromaticity parameters for high-brightness white LED device," *Optics Express*, vol. 29, no. 8, pp. 11938–11946, Apr. 2021, doi: 10.1364/OE.416486.

[14] H. Q. T. Bui *et al.*, "High-performance nanowire ultraviolet light-emitting diodes with potassium hydroxide and ammonium sulfide surface passivation," *Applied Optics*, vol. 59, no. 24, pp. 7352–7356, Aug. 2020, doi: 10.1364/AO.400877.

[15] G. Zhang, K. Ding, G. He, and P. Zhong, "Spectral optimization of color temperature tunable white LEDs with red LEDs instead of phosphor for an excellent IES color fidelity index," *OSA Continuum*, vol. 2, no. 4, pp. 1056–1064, Apr. 2019, doi: 10.1364/OSAC.2.001056.

[16] A. S. Baslamisli and T. Gevers, "Invariant descriptors for intrinsic reflectance optimization," *Journal of the Optical Society of America A*, vol. 38, no. 6, pp. 887–896, Jun. 2021, doi: 10.1364/JOSAA.414682.

[17] G. Granet and J. Bischoff, "Matched coordinates for the analysis of 1D gratings," *Journal of the Optical Society of America A*, vol. 38, no. 6, pp. 790–798, Jun. 2021, doi: 10.1364/JOSAA.422374.

[18] A. Alexeev, J.-P. M. G. Linnartz, K. Arulandu, and X. Deng, "Characterization of dynamic distortion in LED light output for optical wireless communications," *Photonics Research*, vol. 9, no. 6, pp. 916–928, Jun. 2021, doi: 10.1364/PRJ.416269.

[19] I. Fujieda, Y. Tsutsumi, and S. Matsuda, "Spectral study on utilizing ambient light with luminescent materials for display applications," *Optics Express*, vol. 29, no. 5, pp. 6691–6702, Mar. 2021, doi: 10.1364/OE.418869.

[20] N. C. A. Rashid *et al.*, "Spectrophotometer with enhanced sensitivity for uric acid detection," *Chinese Optics Letters*, vol. 17, no. 8, pp. 1–5, 2019, doi: 10.3788/COL201917.081701.

[21] J. Zhou and K. Qian, "Low-voltage wide-field-of-view lidar scanning system based on a MEMS mirror," *Applied Optics*, vol. 58, no. 5, pp. 283–290, Feb. 2019, doi: 10.1364/AO.58.00A283.

[22] Z. Li, J. Zheng, J. Li, W. Zhan, and Y. Tang, "Efficiency enhancement of quantum dot–phosphor hybrid white-light-emitting diodes using a centrifugation-based quasi-horizontal separation structure," *Optics Express*, vol. 28, no. 9, pp. 13279–13289, Apr. 2020, doi: 10.1364/OE.392900.

[23] Y.-P. Chang *et al.*, "New scheme of LiDAR-embedded smart laser headlight for autonomous vehicles," *Optics Express*, vol. 27, no. 20, pp. 1481–1489, Sep. 2019, doi: 10.1364/OE.27.0A1481.

[24] J. Hao, H.-L. Ke, L. Jing, Q. Sun, and R.-T. Sun, "Prediction of lifetime by lumen degradation and color shift for LED lamps, in a non-accelerated reliability test over 20,000 h," *Applied Optics*, vol. 58, no. 7, pp. 1855–1861, Mar. 2019, doi: 10.1364/AO.58.001855.

[25] Z. Huang, Q. Liu, M. R. Pointer, W. Chen, Y. Liu, and Y. Wang, "Color quality evaluation of Chinese bronzeware in typical museum lighting," *Journal of the Optical Society of America A*, vol. 37, no. 4, pp. 170–180, Apr. 2020, doi: 10.1364/JOSAA.381498.
[26] A. Ferrero, B. Bernad, J. Campos, N. Richard, C. Fernández-Maloigne, and M. Melgosa, "Goniochromatic assessment of gray scales for color change," *Journal of the Optical Society of America A*, vol. 37, no. 8, pp. 1266–1275, Aug. 2020, doi: 10.1364/JOSAA.394170.
[27] H.-K. Shih, C.-N. Liu, W.-C. Cheng, and W.-H. Cheng, "High color rendering index of 94 in white LEDs employing novel $CaAlSiN_3$: Eu^{2+} and $Lu_3Al_5O_{12}$:Ce^{3+} co-doped phosphor-in-glass," *Optics Express*, vol. 28, no. 19, pp. 28218–28225, Sep. 2020, doi: 10.1364/OE.403410.
[28] R. Fan, S. Fang, C. Liang, Z. Liang, and H. Zhong, "Controllable one-step doping synthesis for the white-light emission of cesium copper iodide perovskites," *Photonics Research*, vol. 9, no. 5, pp. 694–700, May 2021, doi: 10.1364/PRJ.415015.

BIOGRAPHIES OF AUTHORS

Ha Thanh Tung received the Ph.D. degree in physics from University of Science, Vietnam National University Ho Chi Minh City, Vietnam, he is working as a lecturer at the Faculty of Basic Sciences, Vinh Long University of Technology Education, Vietnam. His research interests focus on developing the patterned substrate with micro-and nano-scale to apply for physical and chemical devices such as solar cells, OLED, and photoanode. He can be contacted at email: tunght@vlute.edu.vn.

Huu Phuc Dang received a Physics Ph.D. degree from the University of Science, Ho Chi Minh City, in 2018. Currently, he is a lecturer at the Faculty of Fundamental Science, Industrial University of Ho Chi Minh City, Ho Chi Minh City, Vietnam. His research interests include simulation LEDs material and renewable energy. He can be contacted at email: danghuuphuc@iuh.edu.vn.

Phung Ton That was born in Thua Thien-Hue, Vietnam. He received the B.Sc. degree in electronics and telecommunications engineering (2007) and the M.Sc. degree in electronics engineering (2010) from the University of Technology, Vietnam. He is currently a lecturer at the Faculty of Electronics Technology (FET), Industrial University of Ho Chi Minh City. His research interests are optical materials, wireless communication in 5G, energy harvesting, performance of cognitive radio, physical layer security, and NOMA. He can be contacted at email: tonthatphung@iuh.edu.vn.